Необичайният случай на един поляриметричен стандарт - възможна причина за променливост при HD 204827

XVIII годишна конференция на Съюза на астрономите в България
15-16 май 2025 г. гр. Белоградчик, България

доц. д-р Янко Николов
Институт по Астрономия с НАО, Българска Академия на Науките
ynikolov@nao-rozhen.org

Стандартни звезди в астрономията

- *Фотометрични стандартни звезди*
- *Спектрофотометрични стандартни звезди*
- *Стандартни звезди за лъчеви скорости*
- *Слънчевите аналози – при изследване на астероиди*
- *Поляриметрични стандартни звезди*

Стандартни звезди в астрономията

Поляриметрични стандартни звезди -- HD 204827

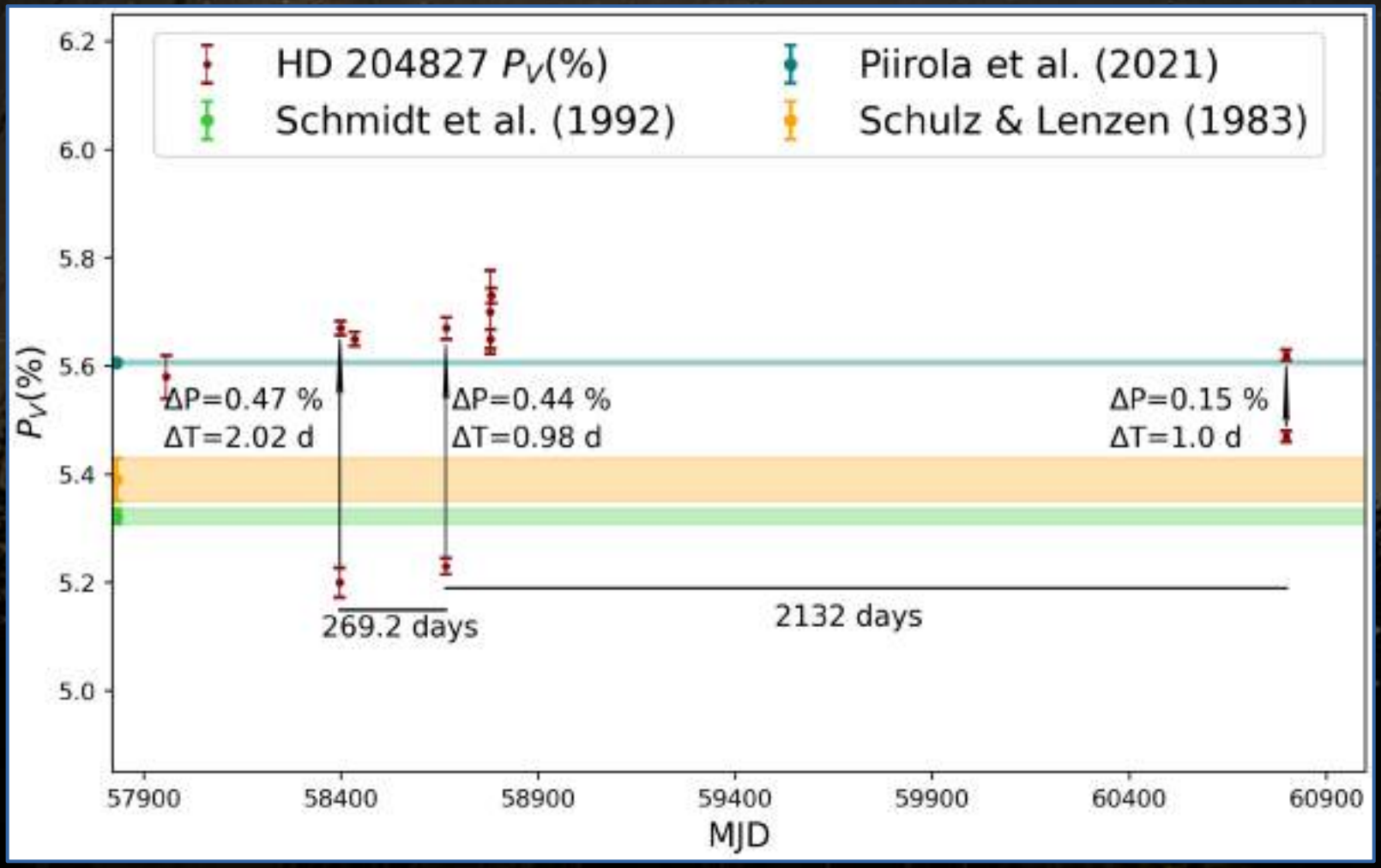

Long-term variability of HD 204827 in the synthetic V-band. The catalogue values are presented with horizontal lines, where the width of each line corresponds to the error of the catalogue value.

Nikolov in prep.

Поляриметрични стандартни звезди

- В двете полукълба има по-малко от **30** звезди със степен на поляризация (PD), известна с точност от 0,1% или по-добра, и за които е доказано, че са стабилни във времето (напр. Schmidt et al. 1992; Hsu & Breger 1982).
- Липсата на подходяща неполяризирана стандартна звезда в нощното небе в даден момент е често срещана.

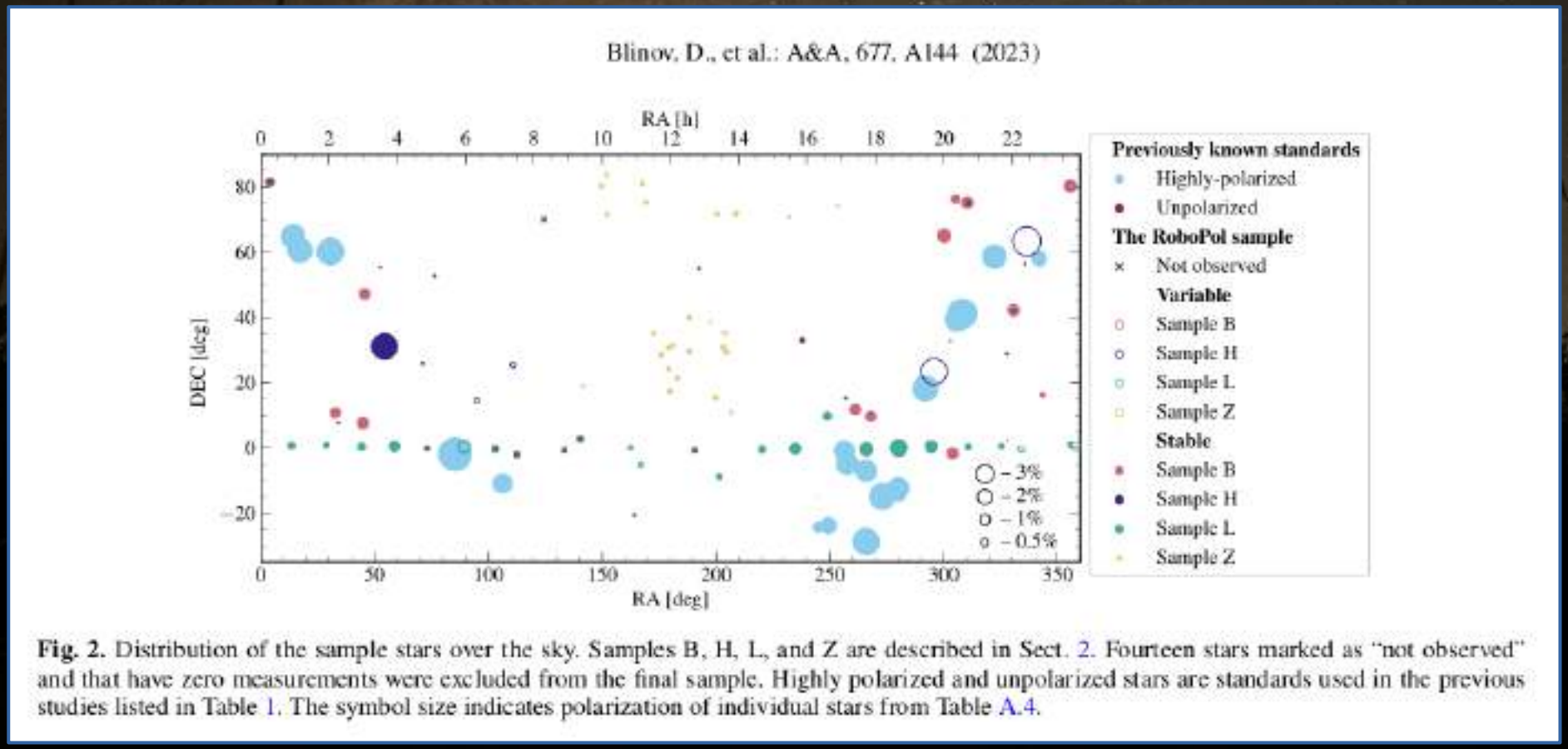

Fig. 2. Distribution of the sample stars over the sky. Samples B, H, L, and Z are described in Sect. 2. Fourteen stars marked as "not observed" and that have zero measurements were excluded from the final sample. Highly polarized and unpolarized stars are standards used in the previous studies listed in Table 1. The symbol size indicates polarization of individual stars from Table A.4.

Blinov + 2023

Спектрополяриметрия с ФоРеРо2





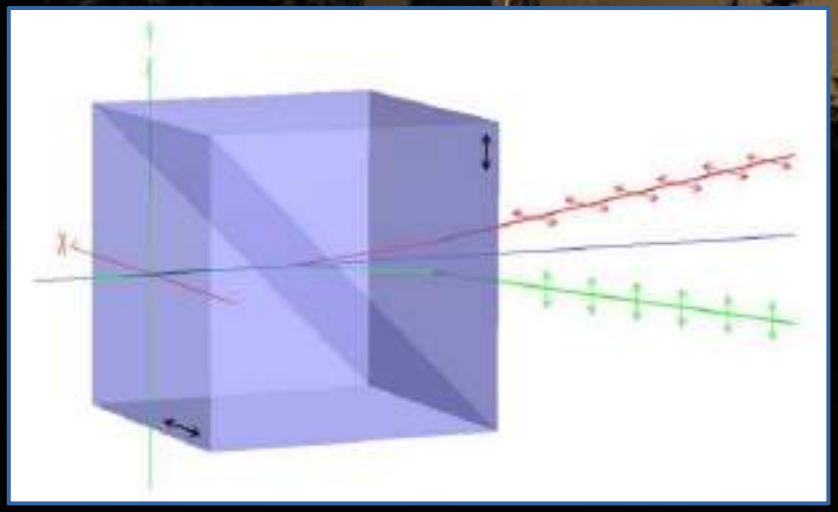

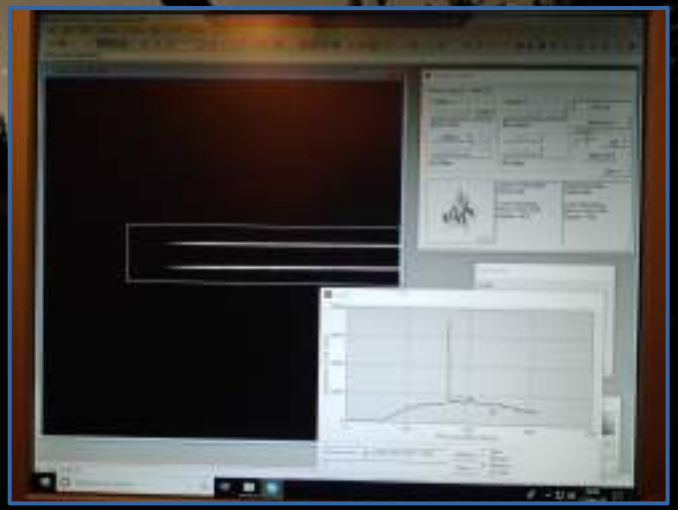

The process of spectropolarimetric data reduction includes:

(1) Bias substraction
(2) Extracting 1D spectra
(3) Wavelength calibration
(4) Beam swapping technique
(5) Correction for instrumental polarization
(6) Correction for the chromatism of the retarder waveplate
(7) Correction for position angle

3.2. Beam swapping technique

A beam swapping technique is used for polarimetric data processing. The values of $f(\lambda)^{\perp}$ and $f(\lambda)^{\parallel}$, where $f(\lambda)^{\parallel}$ and $f(\lambda)^{\perp}$ are the fluxes of the parallel and perpendicular beam of the Wollaston prism respectively, are obtained for the different half-wave retarder plate angles. The following formulae are used to calculate the Stokes parameters (Bagnulo et al. 2009):

$$P_Q(\lambda) = \frac{Q(\lambda)}{I(\lambda)} = \frac{1}{4}\left[\left(\frac{f(\lambda)^{\parallel} - f(\lambda)^{\perp}}{f(\lambda)^{\parallel} + f(\lambda)^{\perp}}\right)_{0^\circ} - \left(\frac{f(\lambda)^{\parallel} - f(\lambda)^{\perp}}{f(\lambda)^{\parallel} + f(\lambda)^{\perp}}\right)_{45^\circ}\right] + \frac{1}{4}\left[\left(\frac{f(\lambda)^{\parallel} - f(\lambda)^{\perp}}{f(\lambda)^{\parallel} + f(\lambda)^{\perp}}\right)_{90^\circ} - \left(\frac{f(\lambda)^{\parallel} - f(\lambda)^{\perp}}{f(\lambda)^{\parallel} + f(\lambda)^{\perp}}\right)_{135^\circ}\right] \quad (1)$$

$$P_U(\lambda) = \frac{U(\lambda)}{I(\lambda)} = \frac{1}{4}\left[\left(\frac{f(\lambda)^{\parallel} - f(\lambda)^{\perp}}{f(\lambda)^{\parallel} + f(\lambda)^{\perp}}\right)_{22.5^\circ} - \left(\frac{f(\lambda)^{\parallel} - f(\lambda)^{\perp}}{f(\lambda)^{\parallel} + f(\lambda)^{\perp}}\right)_{67.5^\circ}\right] + \frac{1}{4}\left[\left(\frac{f(\lambda)^{\parallel} - f(\lambda)^{\perp}}{f(\lambda)^{\parallel} + f(\lambda)^{\perp}}\right)_{112.5^\circ} - \left(\frac{f(\lambda)^{\parallel} - f(\lambda)^{\perp}}{f(\lambda)^{\parallel} + f(\lambda)^{\perp}}\right)_{157.5^\circ}\right] \quad (2)$$

The degree of polarisation is:

$$P_L(\lambda) = \sqrt{P_Q^2(\lambda) + P_U^2(\lambda)}. \quad (3)$$

The position angle is:

$$\theta(\lambda) = \frac{1}{2}\arctan\frac{P_U(\lambda)}{P_Q(\lambda)} + \Theta_0, \quad (4)$$

where Θ_0 is

$$\Theta_0 = \begin{cases} 0^\circ & \text{if } P_Q > 0 \text{ and } P_U \geq 0 \\ 180^\circ & \text{if } P_Q > 0 \text{ and } P_U < 0 \\ 90^\circ & \text{if } P_Q < 0 \end{cases} \quad (5)$$

or

$$\Theta_0 = \begin{cases} 45^\circ & \text{if } P_Q = 0 \text{ and } P_U > 0 \\ 135^\circ & \text{if } P_Q = 0 \text{ and } P_U < 0. \end{cases} \quad (6)$$

Figure 6 presents the Stokes Q and U parameters of the zero polarization standard star HD 154892 before and after application of the beam swapping technique. As Fig. 6 demonstrates, after applying the **BST**, the observed polarization of zero polarization standard is close to zero.

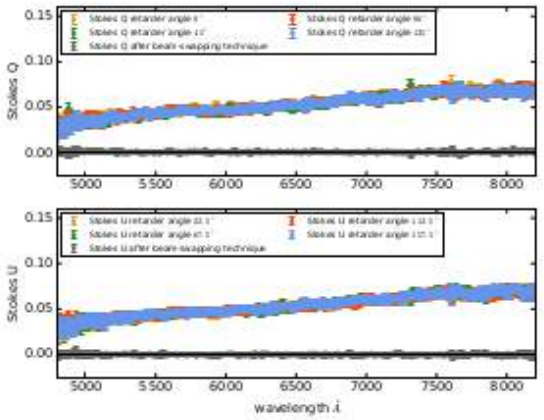

Fig. 6. Stokes Q and U parameter of zero polarization standard star HD 154982 before and after beam swapping technique.

3.3. Instrumental polarization

Regular spectropolarimetric observations started after the installation of the half-wave retarder plate - from November 2015

Unpolarized standard stars

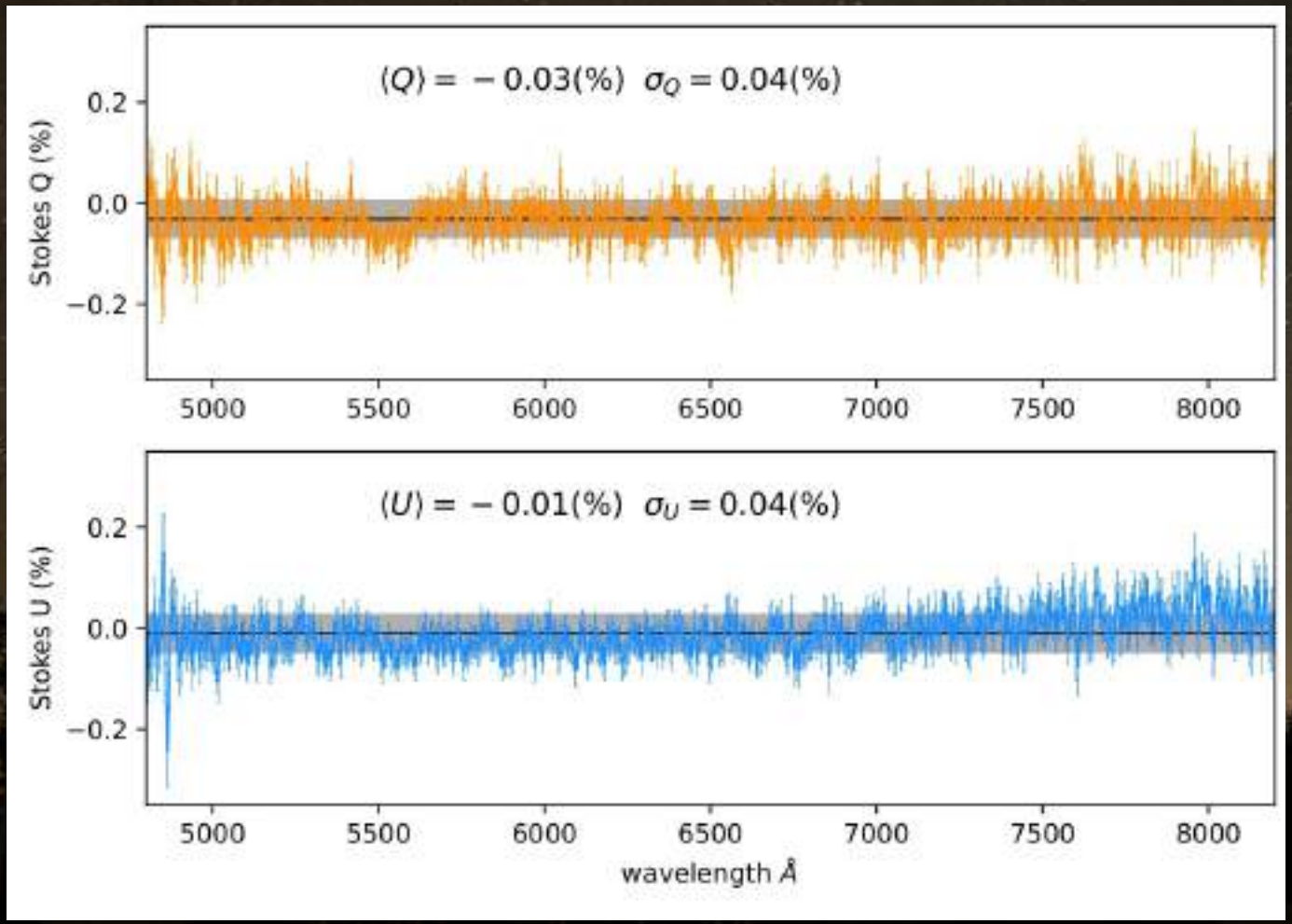

Stokes Q and U parameter of the unpolarized standard star HD 21447

High polarized standard stars

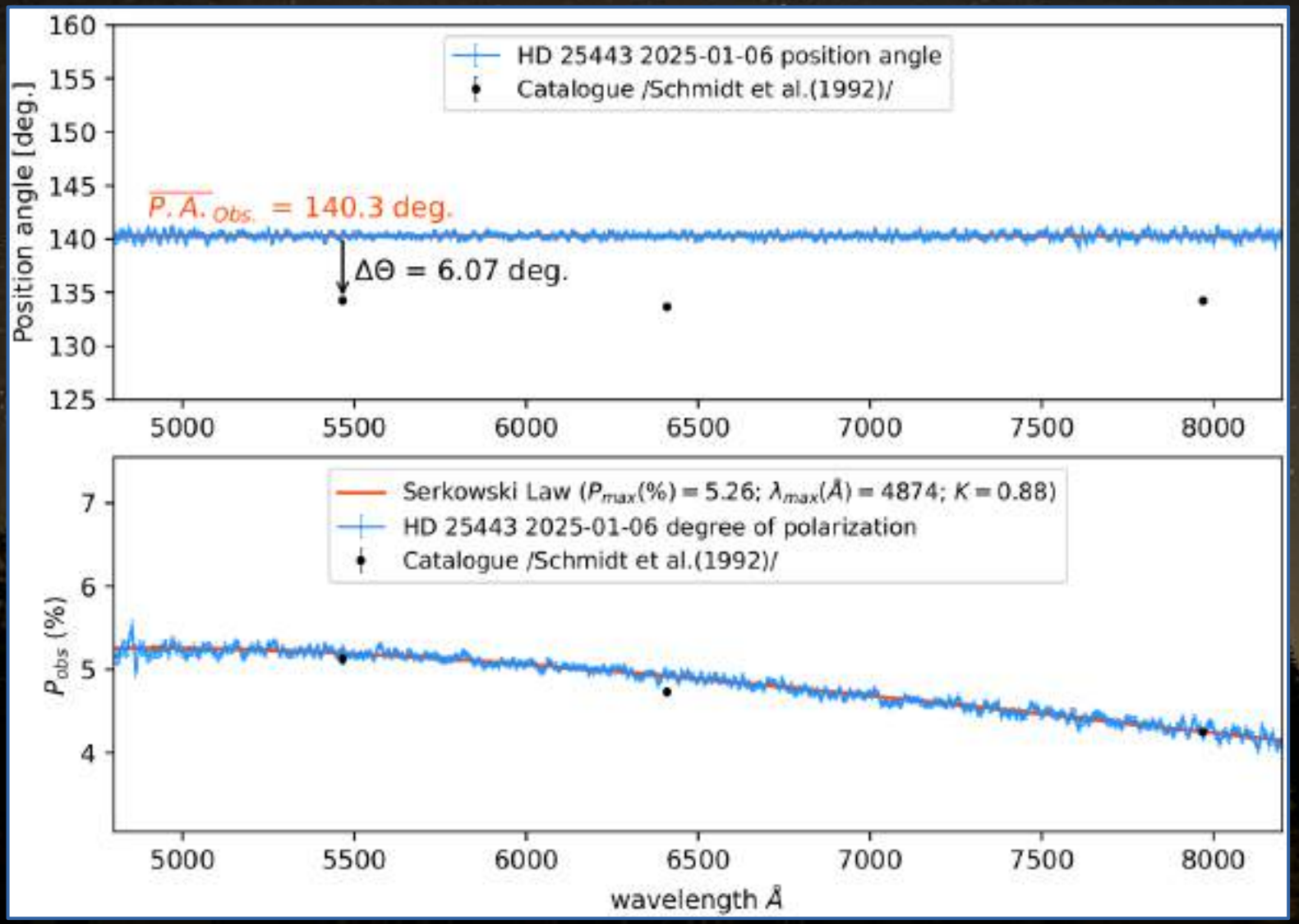

Position angle (top) and degree of polarization (bottom) of the high polarization standard star HD 25443. The black dots represent the catalog value (Schmidt et al., 1992)

Наблюдавани стандарти с ФоРеРо2

6.3. Searching for variability

Usually, the standard deviation is used to determine small fluctuations in magnitude and to detect flickering (e.g., Zamanov et al. (2023)). In this paper, we apply the same idea to detect the variability of high-polarization standard stars.

The standard deviation is calculated as:

$$\sigma_{rms} = \sqrt{\frac{1}{N_{pts}-1}\sum_{i}(P_V(i)-\overline{P}_V)^2}, \quad (19)$$

Table 1: List of spectropolarimetric observed standard stars. The coordinates were taken from the SIMBAD Astronomical Database.

Name	R.A. (J2000)	Dec. (J2000)	N° of obs.	$\overline{P_V}$ (%)	$\sigma_{rms}(P_V)$ (%)	Band	P.D. (%) (catalogue)	P.A. (deg.) (catalogue)	References
Unpolarised standard stars									
HD 191195	20 06 13.9	+53 09 56.5	8	0.03	0.01	-	0.0039 ± 0.0008	68.2 ± 5.6	(b)
HD 21447	03 30 00.2	+55 27 06.5	16	0.05	0.02	V	0.051 ± 0.020	171.49	(a)
HD 154892	17 07 41.3	+15 12 37.6	21	0.08	0.04	B	0.050 ± 0.030	-	(c)
HD 212311	22 21 58.6	+56 31 52.7	10	0.11	0.03	V	0.034 ± 0.021	50.99	(a)
High polarisation standards									
HD 7927	01 20 04.9	+58 13 53.8	3	3.25	0.08	V	3.298 ± 0.025	91.08 ± 0.2	(a)
HD 25443	04 06 08.1	+62 06 06.6	14	5.21	0.05	V	5.127 ± 0.061	134.23 ± 0.34	(a)
HD 161056	17 43 47.0	-07 04 46.6	27	4.05	0.04	V	4.030 ± 0.025	66.93 ± 0.18	(a)
HD 19820	03 14 05.3	+59 33 48.5	11	4.82	0.03	V	4.787 ± 0.028	114.93 ± 0.17	(a)
BD +25 727	04 44 24.9	+25 31 42.4	2	6.31	–	V	6.28 ± 0.003	32.2 ± 0.1	(f)
BD +59 389	02 02 42.1	+60 15 26.4	2	6.63	–	V	6.701 ± 0.015	98.09 ± 0.07	(a)
HD 154445	17 05 32.3	-00 53 31.4	3	3.72	0.06	V	3.780 ± 0.062	88.79 ± 0.47	(a)
HD 155197	17 10 15.8	-04 50 03.7	1	4.45	–	V	4.320 ± 0.023	102.84 ± 0.15	(a)
Variable high polarisation standards									
HD 183143	19 27 26.6	+18 17 45.2	7	6.13	**0.15**	V	6.10 ± 0.05	179.3 ± 0.2	(d)
HD 204827	21 28 57.8	+58 44 23.2	9	5.56	**0.20**	V	5.322 ± 0.014	58.73 ± 0.08	(a)
						V	5.607 ± 0.003	58.33 ± 0.02	(e)

Note: (a) Schmidt et al. (1992); (b) Piirola et al. (2020); (c) Turnshek et al. (1990); (d) Hsu & Breger (1982); (e) Piirola et al. (2021); (f) Nordic Optical Telescope[5].

Nikolov + in prep.

Променливи стандартни звезди

55 Cyg (HD 198478), HD43384 и HD183143 (Hsu & Breger 1982)

7 от 13 стандарта са променливи (Bastien + 2007)

Променливост в позиционния ъгъл е намерен при 5 стандарта: HD 160529, HD 80558, HD 111613, HD 183143 и 55 Cyg (Cotton + 2024)

HD 204827 – променливост в позиционния ъгъл (this work)

Звезди с висока поляризация

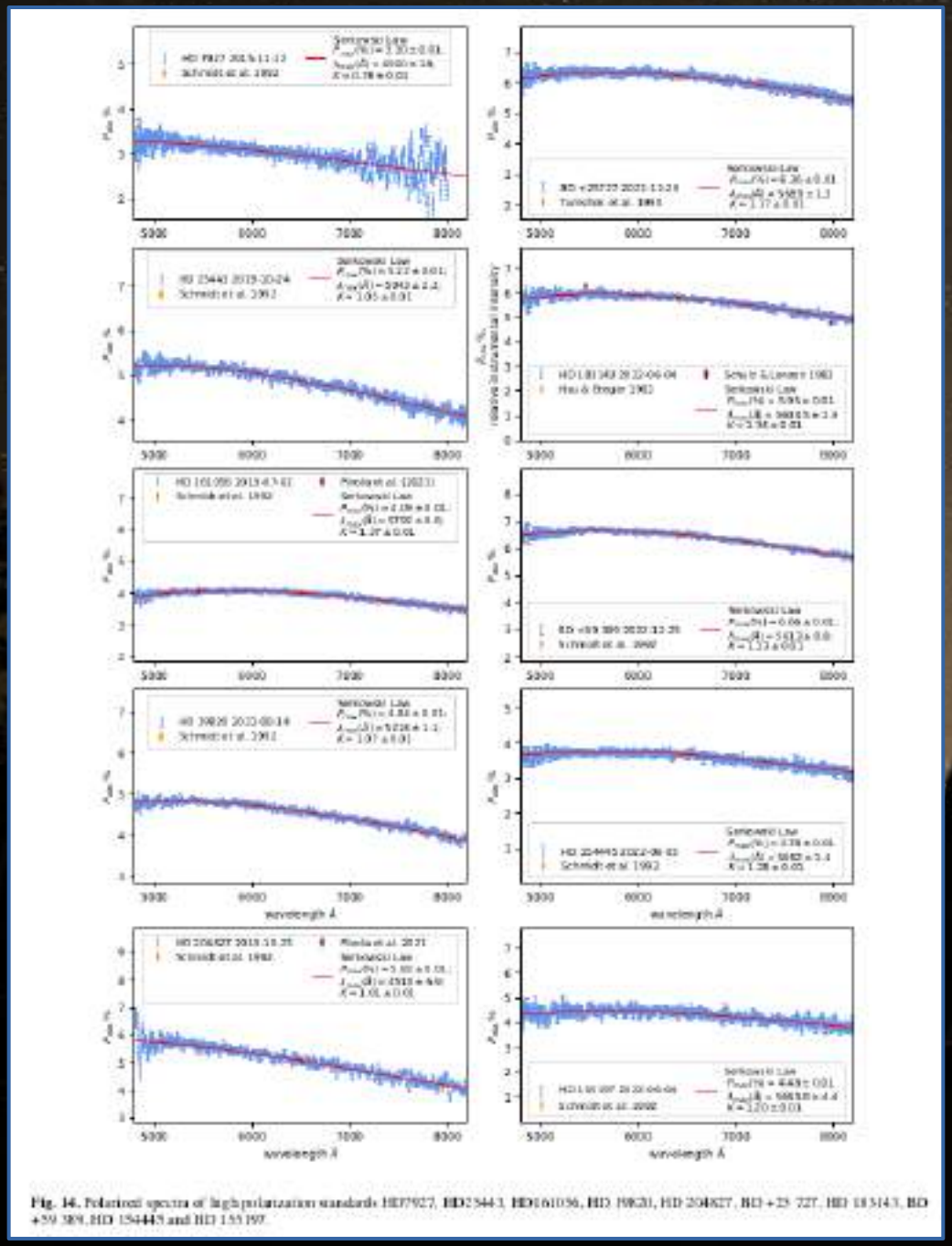

Fig. 14. Polarized spectra of high polarization standards HD7927, HD25443, HD161056, HD 19820, HD 204827, BD +25 727, HD 183143, BD +59 389, HD 154445 and HD 155197.

Закон на Серковски

$$P_{IS}\,p(\lambda) = P_{max}\ \exp\left(-K \ln^2 \frac{\lambda_{max}}{\lambda}\right),$$

Table 3. The parameters of the Serkowski's law fit.

Object	The parameters of the Serkowski's law fit		
	$P(\lambda)_{max}$ (%)	K	λ_{max} (Å)
HD 7927	3.30 ± 0.01	0.78 ± 0.01	4500 ± 18
HD 25443	5.22 ± 0.01	1.05 ± 0.01	5043 ± 2.3
HD 161056	4.09 ± 0.01	1.37 ± 0.01	5792 ± 0.6
HD 19820	4.84 ± 0.01	1.07 ± 0.01	5218 ± 1.1
HD 204827	5.83 ± 0.01	1.01 ± 0.01	4510 ± 6.9
BD +25 727	6.36 ± 0.01	1.17 ± 0.01	5689 ± 1.3
HD 183143	5.95 ± 0.01	1.34 ± 0.01	5604 ± 1.3
BD +59 389	6.66 ± 0.01	1.13 ± 0.01	5613 ± 0.8
HD 154445	3.78 ± 0.01	1.28 ± 0.01	5662 ± 1.4
HD 155197	4.48 ± 0.01	1.20 ± 0.01	5664 ± 4.4

Nikolov + in prep.

HD 204827 -- Spectroscopic Binary

HD204827 is classified as a spectroscopic binary star with an unknown period, as both components exhibit spectral types close to O9.5 V or B0 V (Hobbs et al. 2008).

TESS light curve

The light curves from the Transiting Exoplanet Survey Satellite (TESS) mission were extracted using TESSExtractor-- https://www.tessextractor.app/

TESS observed HD 204827 during eight sectors (Sectors 16, 17, 56, 57, 76, 77, 83, and 84). The light curve exhibits the same structure across all sectors.

The light curve is similar to those of eclipsing binary stars but has very shallow minima. Light curves of eclipsing binary stars can be found in the TESS Eclipsing Binary Stars Catalogue (Prša et al. 2022).

Nikolov in prep.

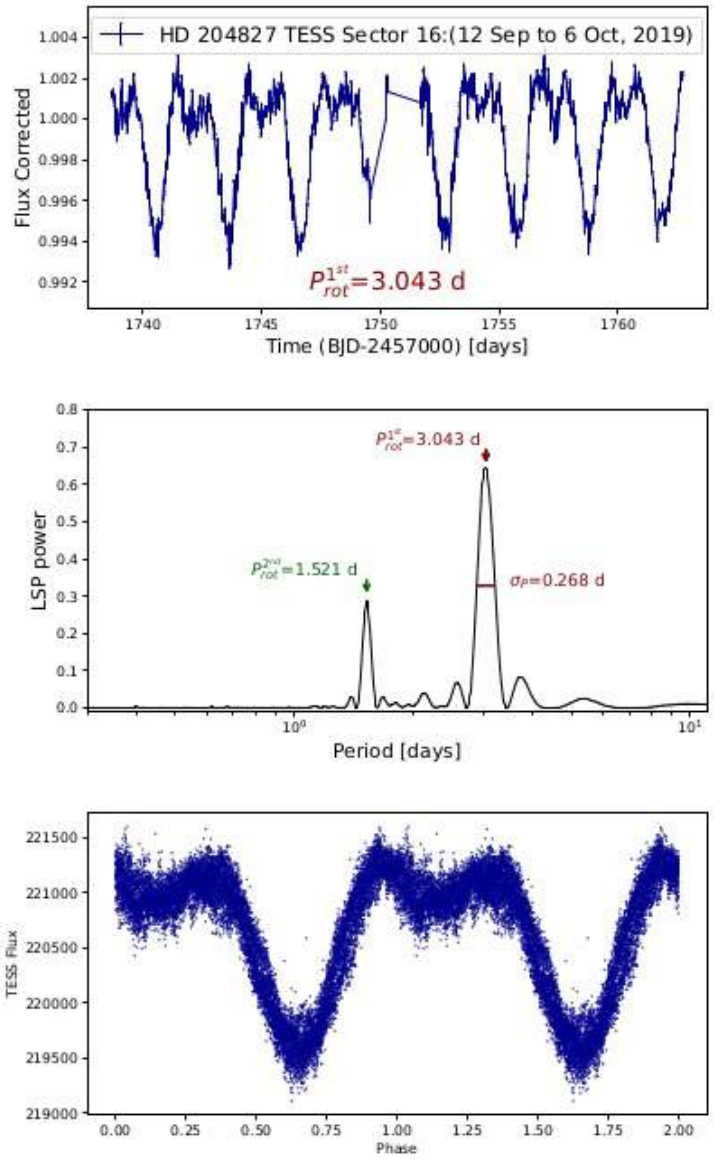

Fig. 21: TESS light curve (top), Lomb-Scargle periodogram (middle), and phase-folded light curve based on the most significant period detected from the periodogram (bottom).

HD 204827

The variation in the degree of polarization is not related to the orbital period!

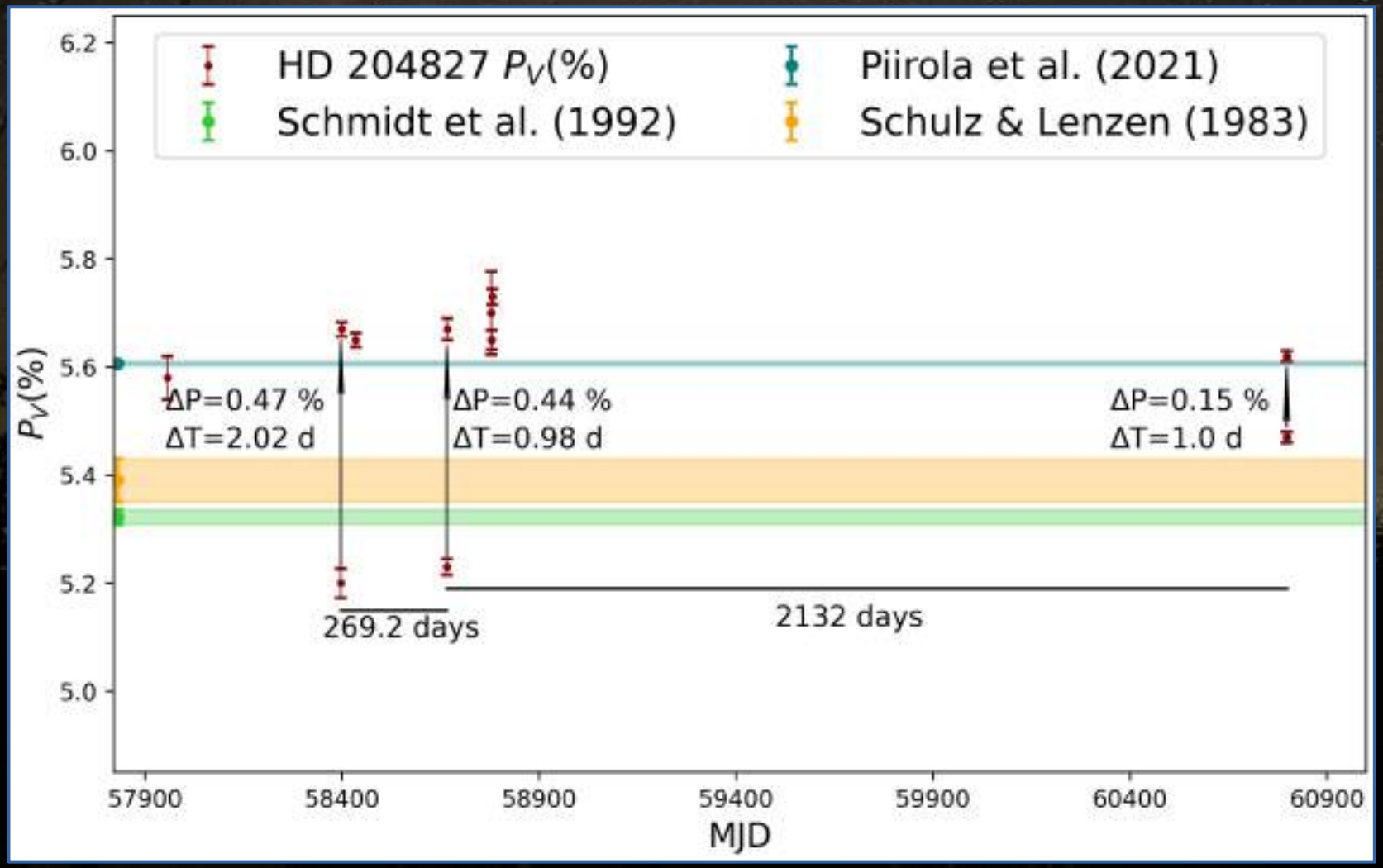

Long-term variability of HD 204827 in the synthetic V-band. The catalogue values are presented with horizontal lines, where the width of each line corresponds to the error of the catalogue value.

Nikolov in prep.

Steps to analyze spectropolarimetric data

1)Variable polarization – an indicator of asymmetry

2)Determine the intrinsic and interstellar polarization

3)Analyze the wavelength dependence of the degree of polarization

4)Determine the orientation of the position angle

5)Measure the polarized flux across the Hα emission line

Interstellar polarization toward HD 204827

Interstellar polarization toward HD 204827

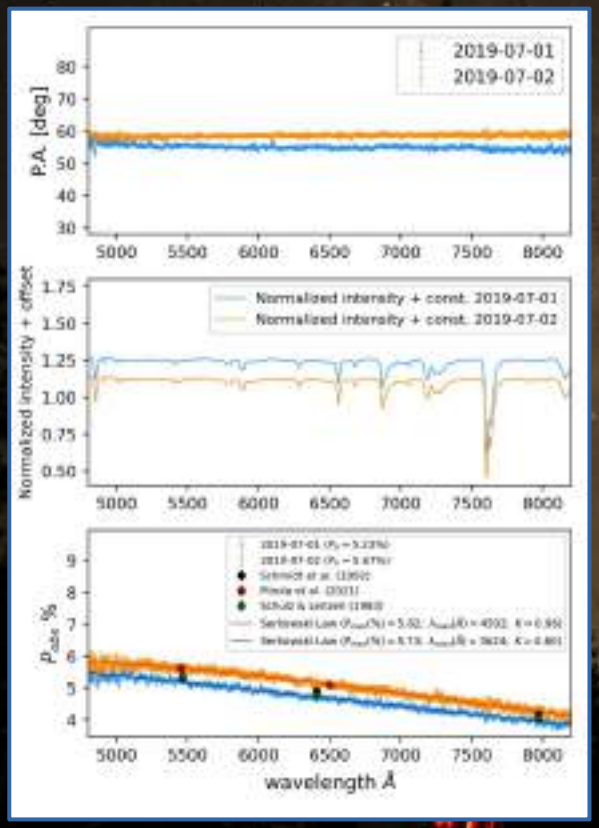

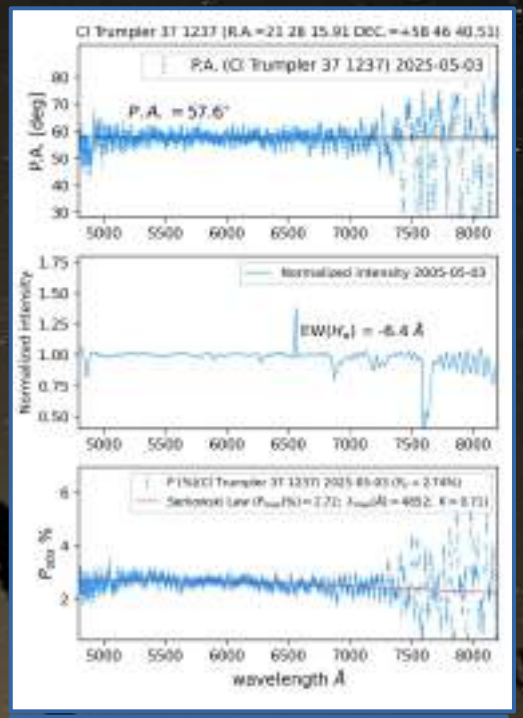

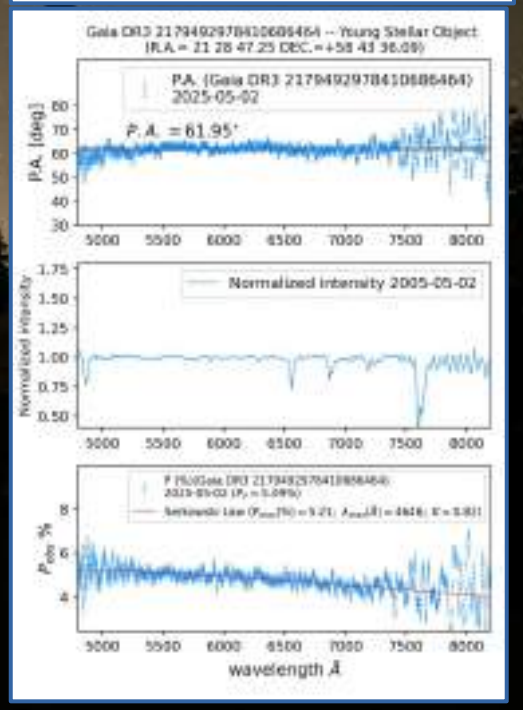

Nikolov in prep.

Interstellar polarization toward HD 204827

HD 204827 , distance = 918 pc
Cl Trumpler 37 1237, distance = 1027 pc, angular distance = 5.9’
Gaia DR3 2179492978410686464, distance = 903 pc, angular distance = 1.6’

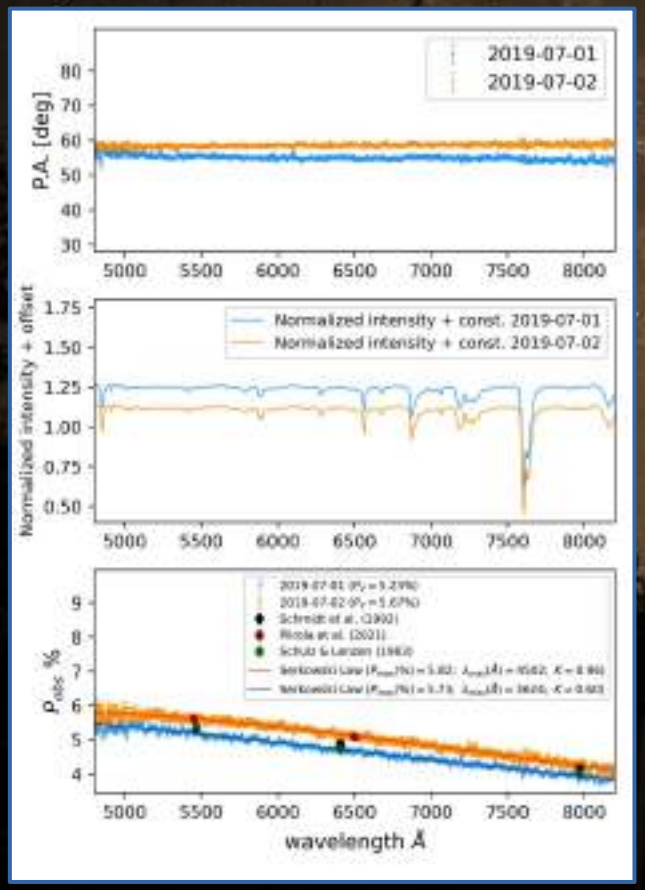

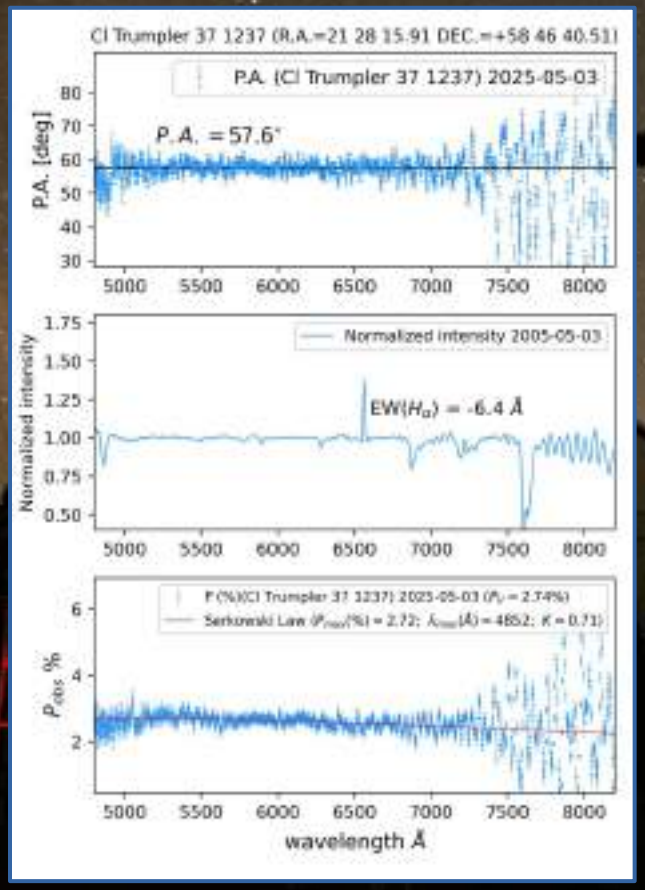

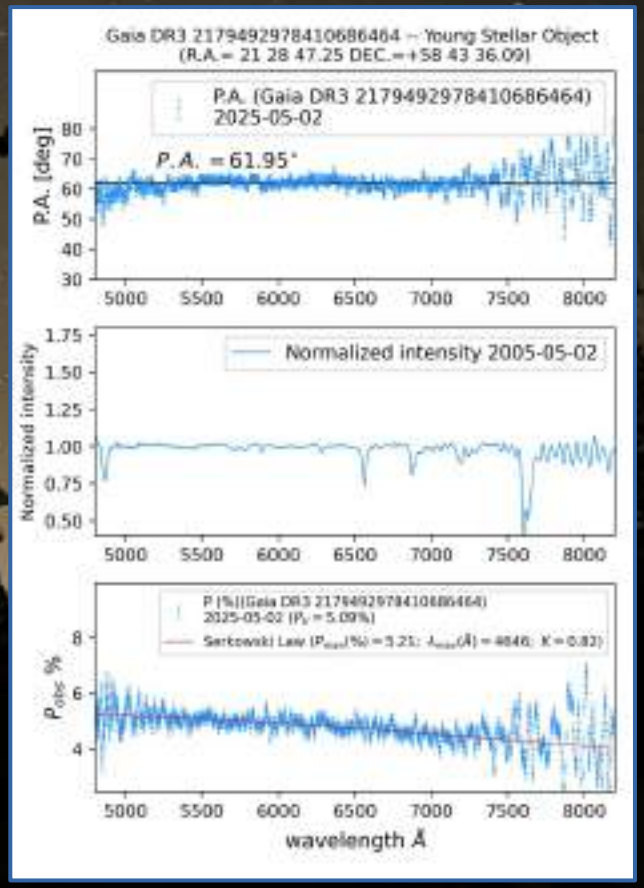

Observed P.A. , instrumental intensity and degree of polarization of HD 204827 and two stars in the vicinity of the HD 204827. Nikolov in prep.

Polarization vs. distance

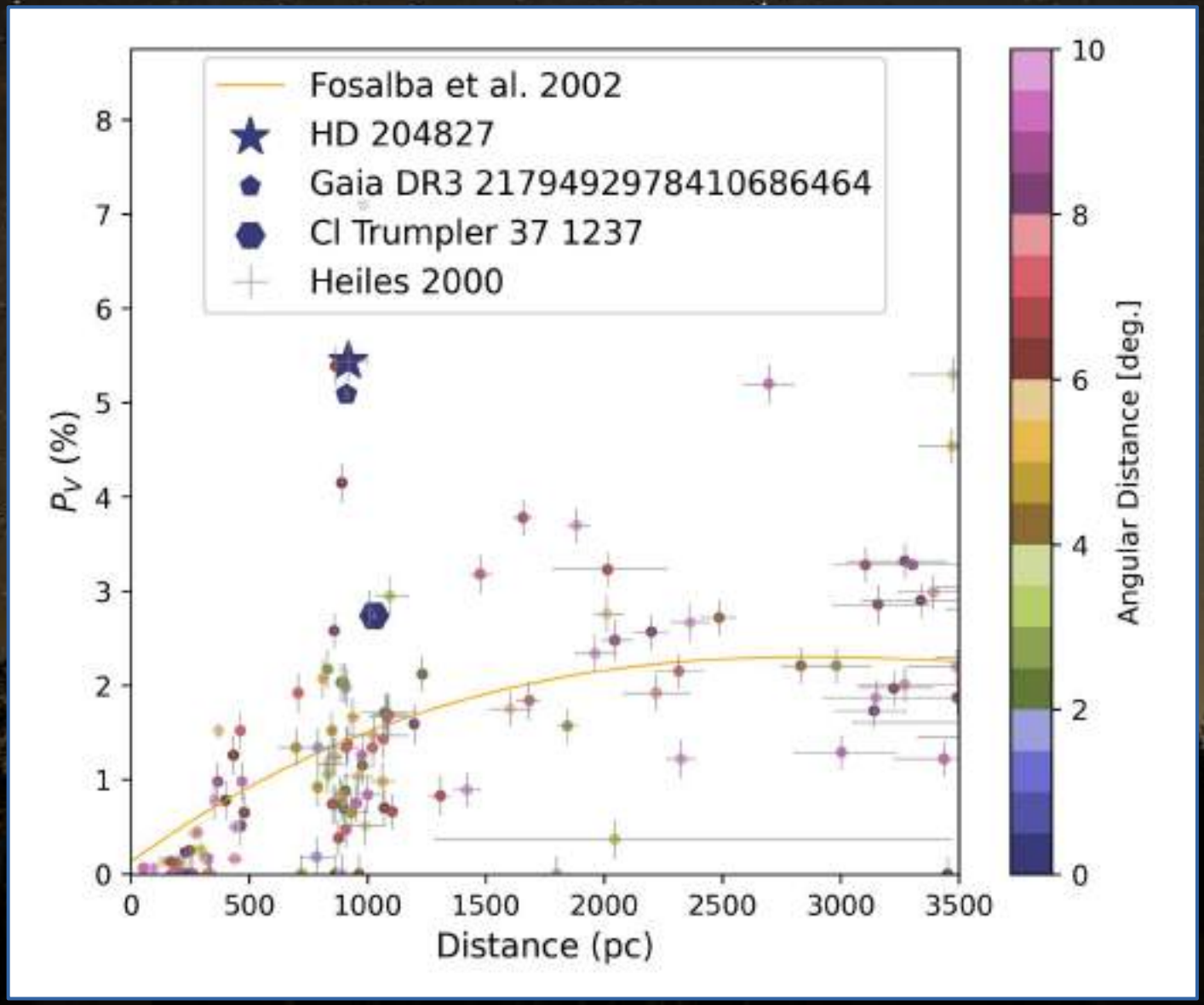

Polarization vs. distance. The orange line represents the polarization vs. distance relationship (Fosalba et al. 2002).

3D polarization map around HD 204827

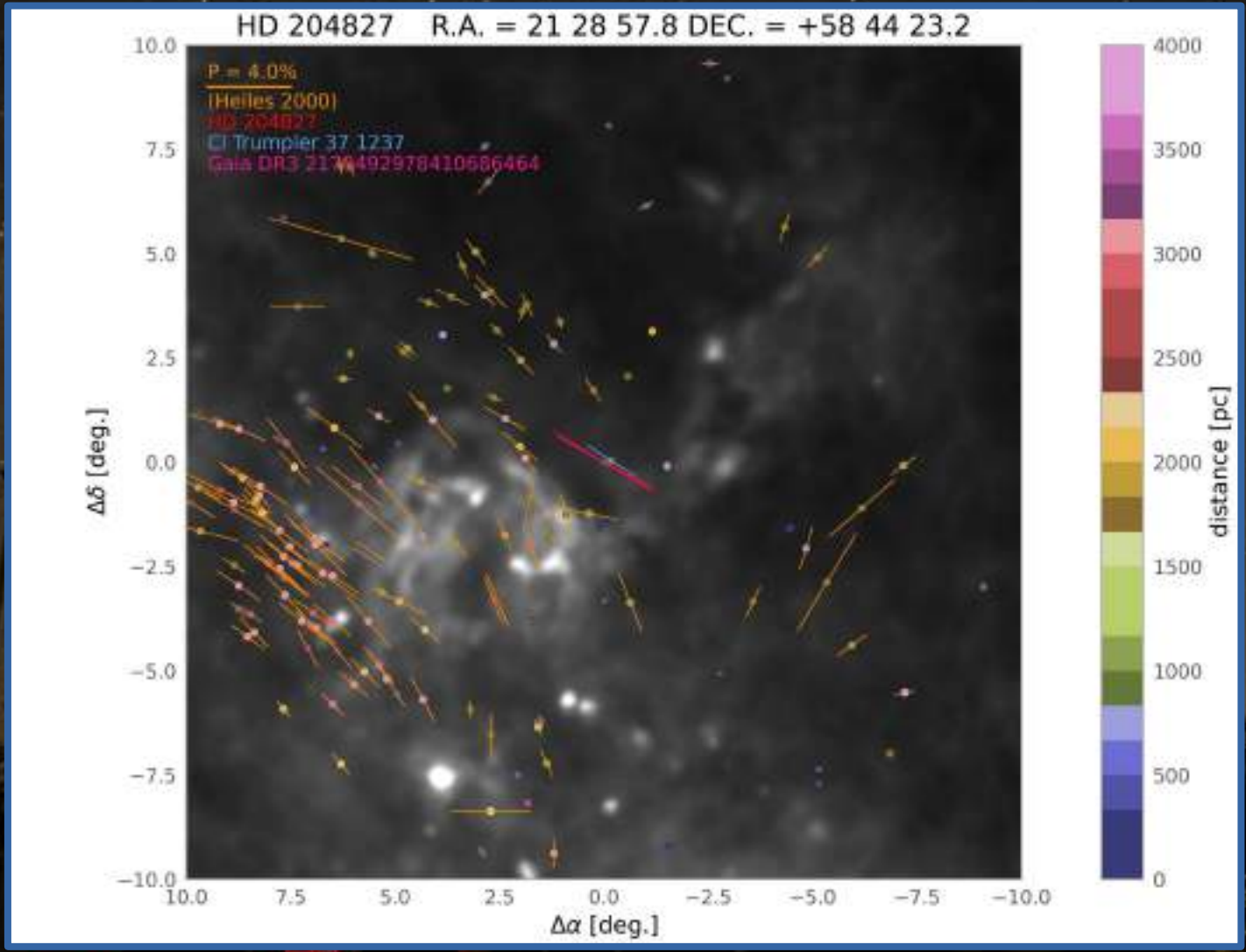

The interstellar polarization of the field stars around HD 204827 (with orange,Heiles (2000)). The degree of polarization is proportional to the length of its bar. The horizontal bar of the top right presents 4 % polarization. The P.A. of the stars of the direction of HD 204827 are similar to that observed in HD 204827. The color of every star corresponds to its distance. The background image represents 100 μm dust emission maps (Schlegel et al., 1998).

HD 204827 has an IRAS bow shock

THE ASTROPHYSICAL JOURNAL, 598:369–374, 2003 November 20

SMALL MAGELLANIC CLOUD–TYPE INTERSTELLAR DUST IN THE MILKY WAY

LYNNE A. VALENCIC,[1] GEOFFREY C. CLAYTON,[1] KARL D. GORDON,[2] AND TRACY L. SMITH[3]

Received 2003 June 4; accepted 2003 August 1

ABSTRACT

It is well known that the sight line toward HD 204827 in the cluster Trumpler 37 shows a UV extinction curve that does not follow the average Galactic extinction relation. However, when a dust component, foreground to the cluster, is removed, the residual extinction curve is identical to that found in the SMC within the uncertainties. The curve is very steep and has little or no 2175 Å bump. The position of HD 204827 in the sky is projected onto the edge of the Cepheus *IRAS* bubble. In addition, HD 204827 has an *IRAS* bow shock, indicating that it may be embedded in dust swept up by the supernova that created the *IRAS* bubble. Shocks due to the supernova may have led to substantial processing of this dust. The HD 204827 cloud is dense and rich in carbon molecules. The 3.4 μm feature indicating a C-H grain mantle is present in the dust toward HD 204827. The environment of the HD 204827 cloud dust may be similar to the dust associated with HD 62542, which lies on the edge of a stellar wind bubble and is also dense and rich in molecules. This sight line may be a Rosetta Stone if its environment can be related to those in the SMC having similar dust.

Subject headings: dust, extinction — Magellanic Clouds

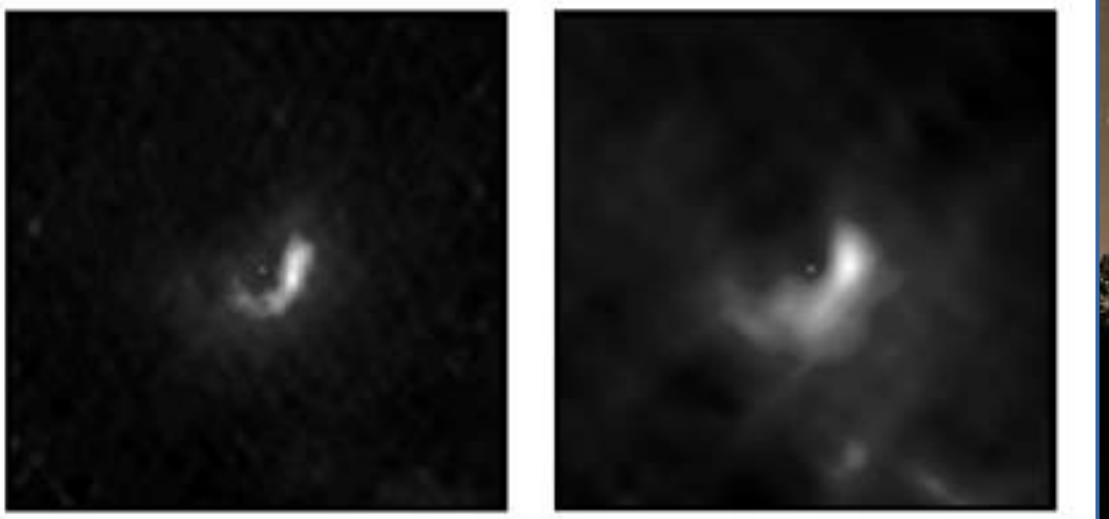

FIG. 3.—4'.5 × 0'.5 *IRAS* HiRes images of HD 204827 at 25 (*left*) and 60 μm (*right*). The cross indicates the star's location.

"Since the uncertainty in the velocity is rather large, we can only say that the velocity HD 204827 is consistent with being a **runaway star**."

Valencic + 2003

"The presence of the bow shock around HD 204827 indicates that the star may lie in or near the material swept up in the formation of the bubble. It formed through a combination of stellar winds and a supernova explosion from the first generation of star formation in the region, NGC 7160, which occurred about 7 Myr ago (Patel et al. 1998). The Trumpler 37 cluster formed about 5 Myr ago perhaps induced by the formation of the Cepheus bubble. Shocks such as those in supernova ejecta will produce a dust grain size distribution skewed toward smaller grains."

Valencic + 2003

STELLAR BOWSHOCK NEBULAE IN THE MILKY WAY

A COMPREHENSIVE SEARCH FOR STELLAR BOWSHOCK NEBULAE IN THE MILKY WAY: A CATALOG OF 709 MID-INFRARED SELECTED CANDIDATES Kobulnicky + 2016

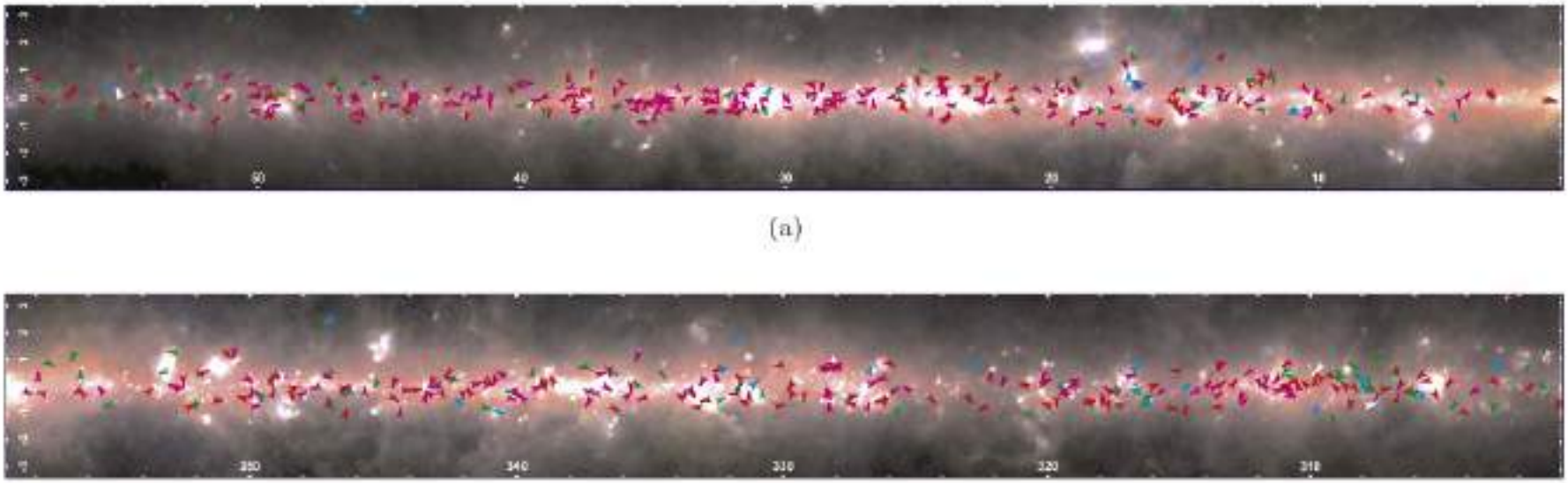

(a)

(b)

Figure 4. Locations of bowshock candidates drawn as arrows to indicate the morphological orientation of the nebula. Colors designate interstellar extinction values, just as in Figure 2. The upper panel shows a portion of the Plane at $0^\circ < \ell < 60^\circ$, while the lower panel shows the $300^\circ < \ell < 360^\circ$ region.

Kobulnicky + 2016

STELLAR BOWSHOCK NEBULAE IN THE MILKY WAY

A COMPREHENSIVE SEARCH FOR STELLAR BOWSHOCK NEBULAE IN THE MILKY WAY: A CATALOG OF 709 MID-INFRARED SELECTED CANDIDATES Kobulnicky + 2016

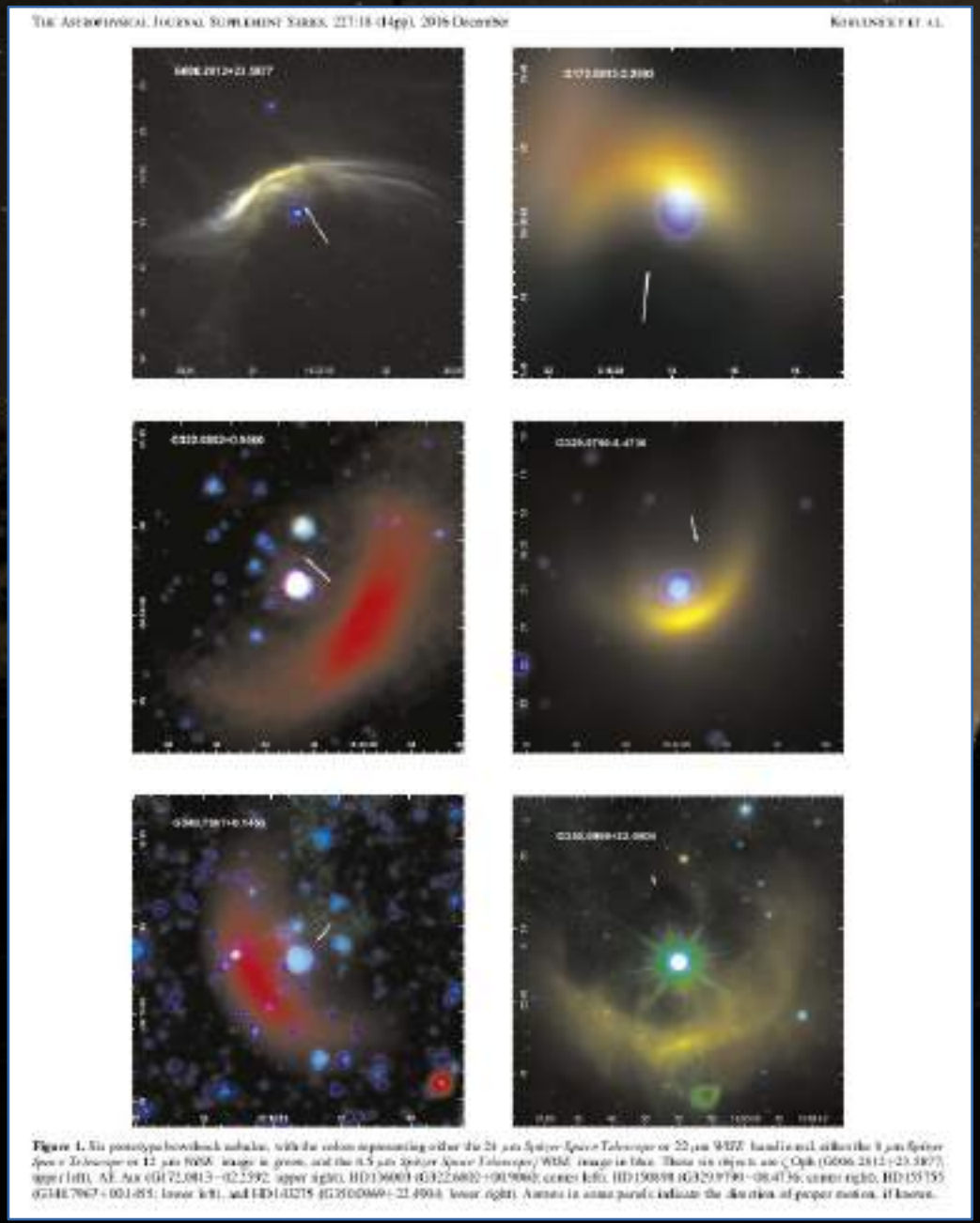

Six prototype bowshock nebulae, with the colors representing either the 24 μm Spitzer Space Telescope or 22 μm WISE band in red, either the 8 μm Spitzer Space Telescope or 12 μm WISE image in green, and the 4.5 μm Spitzer Space Telescope/WISE image in blue. These six objects are ζ Oph (G006.2812+23.5877; upper left), AE Aur (G172.0813−02.2592; upper right), HD136003 (G322.6802+00.9060; center left), HD150898 (G329.9790−08.4736; center right), HD155755 (G348.7967+00.1455; lower left), and HD143275 (G350.0969+22.4904; lower right). Arrows in some panels indicate the direction of proper motion, if known.

Kobulnicky + 2016

Theory

Monthly Notices of the ROYAL ASTRONOMICAL SOCIETY

MNRAS **477,** 1365–1382 (2018) doi:10.1093/mnras/sty724
Advance Access publication 2018 March 20

Polarization simulations of stellar wind bow-shock nebulae – I. The case of electron scattering

Manisha Shrestha,[1]★ Hilding R. Neilson,[2] Jennifer L. Hoffman[1] and Richard Ignace[3]

[1]*Department of Physics and Astronomy, University of Denver, 2112 E. Wesley Ave., Denver, CO 80208, USA*
[2]*Department of Astronomy and Astrophysics, University of Toronto, 50 St George Street, Toronto, ON M5S 3H4, Canada*
[3]*Department of Physics and Astronomy, East Tennessee State University, Johnson City, TN 37614, USA*

Monthly Notices of the ROYAL ASTRONOMICAL SOCIETY

MNRAS **500,** 4319–4337 (2021) doi:10.1093/mnras/staa3508
Advance Access publication 2020 November 12

Polarization simulations of stellar wind bow shock nebulae – II. The case of dust scattering

Manisha Shrestha ,[1,2]★ Hilding R. Neilson,[3] Jennifer L. Hoffman ,[1] Richard Ignace[4] and Andrew G. Fullard[1]

[1]*Department of Physics & Astronomy, University of Denver, 2112 E Wesley Ave., 80208, Denver, USA*
[2]*Astrophysics Research Institute, Liverpool John Moores University, 146 Brownlow Hill, Liverpool L3 5RF, UK*
[3]*Department of Astronomy & Astrophysics, University of Toronto, 50 St. George Street, M5S 3H4, Toronto, Canada*
[4]*Department of Physics & Astronomy, East Tennessee State University, Johnson City, TN 37614, USA*

Theory

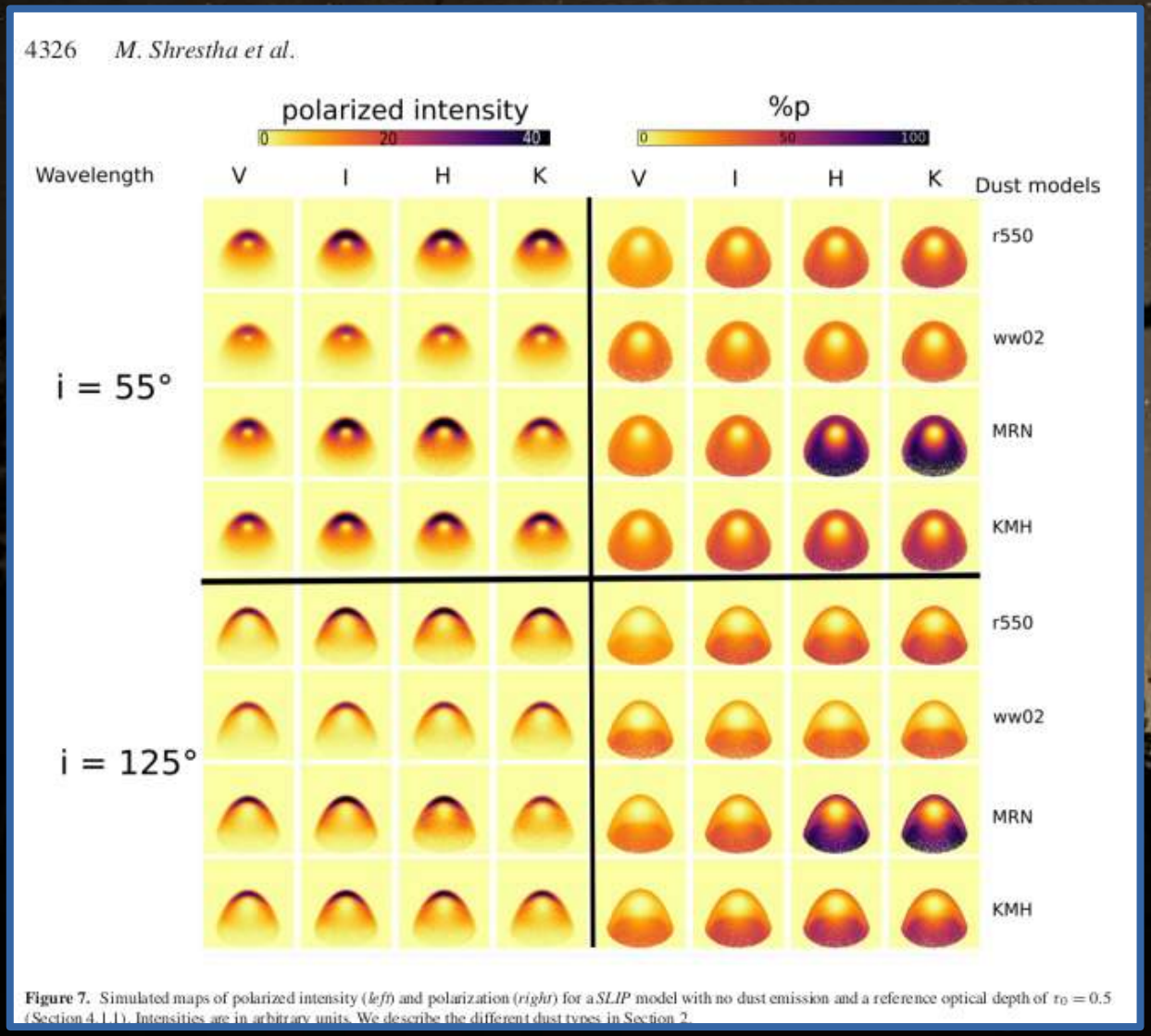

Figure 7. Simulated maps of polarized intensity (*left*) and polarization (*right*) for a *SLIP* model with no dust emission and a reference optical depth of $\tau_0 = 0.5$ (Section 4.1.1). Intensities are in arbitrary units. We describe the different dust types in Section 2.

The resulting polarization is highly dependent on the inclination angle, wavelength, and dust grain properties.
Shrestha +

Theory

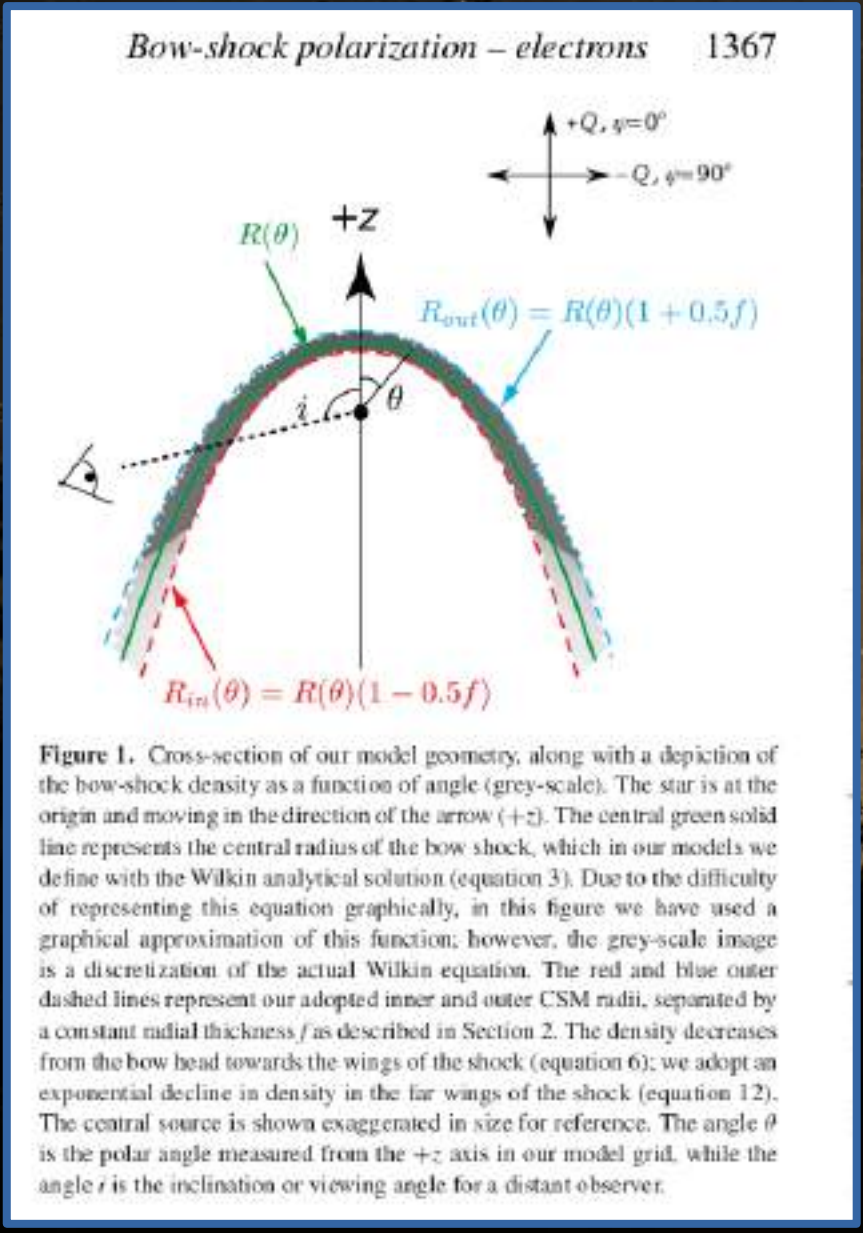

Figure 1. Cross-section of our model geometry, along with a depiction of the bow-shock density as a function of angle (grey-scale). The star is at the origin and moving in the direction of the arrow (+z). The central green solid line represents the central radius of the bow shock, which in our models we define with the Wilkin analytical solution (equation 3). Due to the difficulty of representing this equation graphically, in this figure we have used a graphical approximation of this function; however, the grey-scale image is a discretization of the actual Wilkin equation. The red and blue outer dashed lines represent our adopted inner and outer CSM radii, separated by a constant radial thickness *f* as described in Section 2. The density decreases from the bow head towards the wings of the shock (equation 6); we adopt an exponential decline in density in the far wings of the shock (equation 12). The central source is shown exaggerated in size for reference. The angle θ is the polar angle measured from the +z axis in our model grid, while the angle *i* is the inclination or viewing angle for a distant observer.

"The position angles in our models are consistently ≈0◦ for most viewing angles, but flip to near 90◦ at high inclinations and optical depths when q is negative."

"Polarization simulations of stellar wind bow-shock nebulae – I. The case of electron scattering"
Shrestha + 2018

A peek behind the dusty curtain: K S -band polarization photometry and bow shock models of the Galactic center source IRS 8

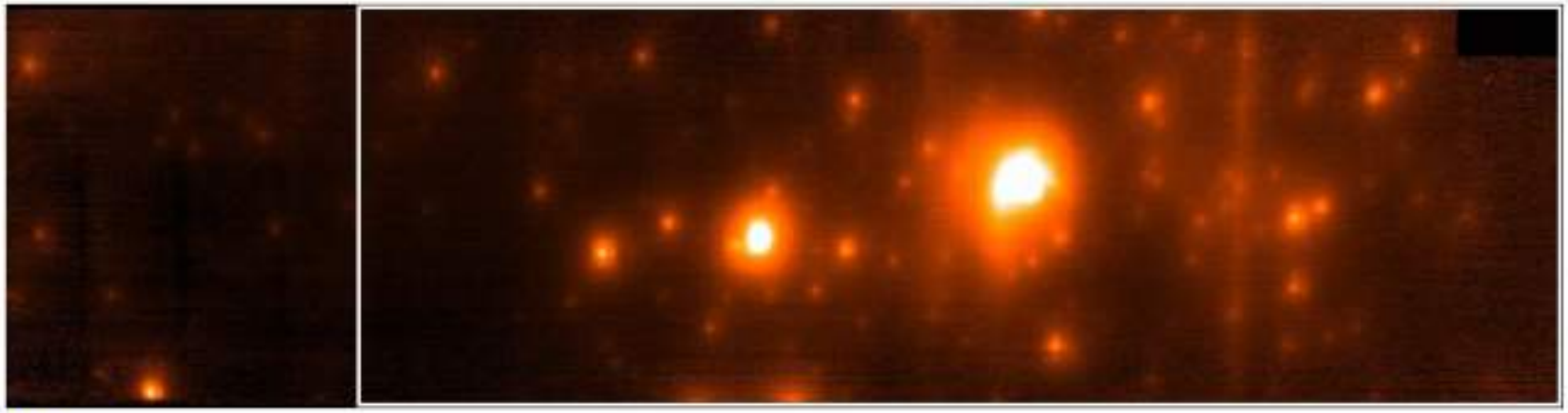

Fig. 1. K_S-band FOV for one Wollaston channel covering an area of 31.9″ × 8.2″. The white box marks the area used for the presented polarization maps.

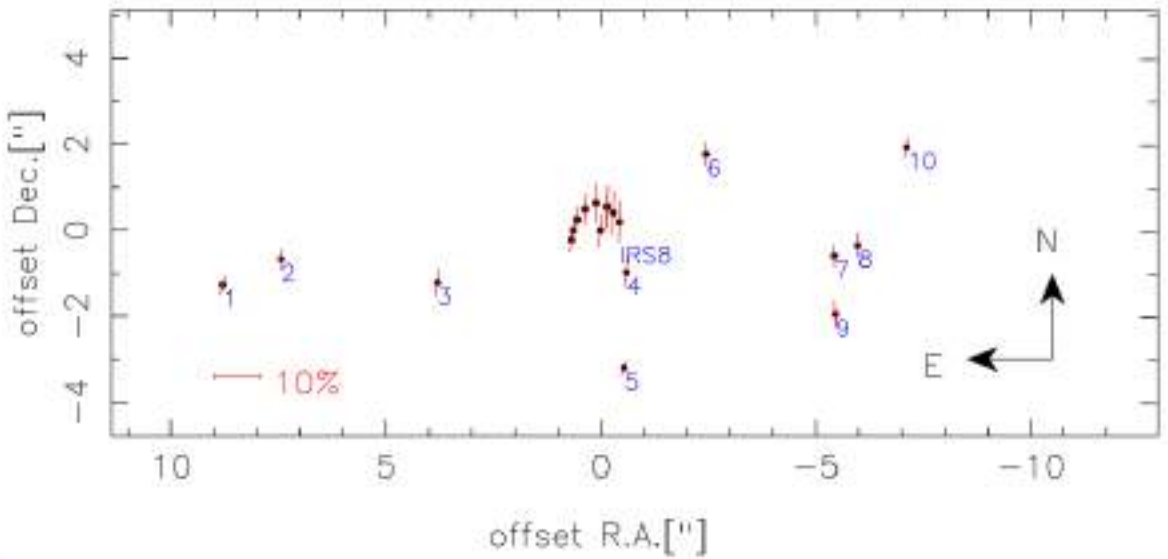

Fig. 2. Polarization map of IRS 8 and its surrounding sources. Polarization was measured on nondeconvolved images using the techniques described in Sect. 2. The images were not corrected for background flux or foreground and instrumental polarization.

Rauch + 2013

HD 204827- position angle

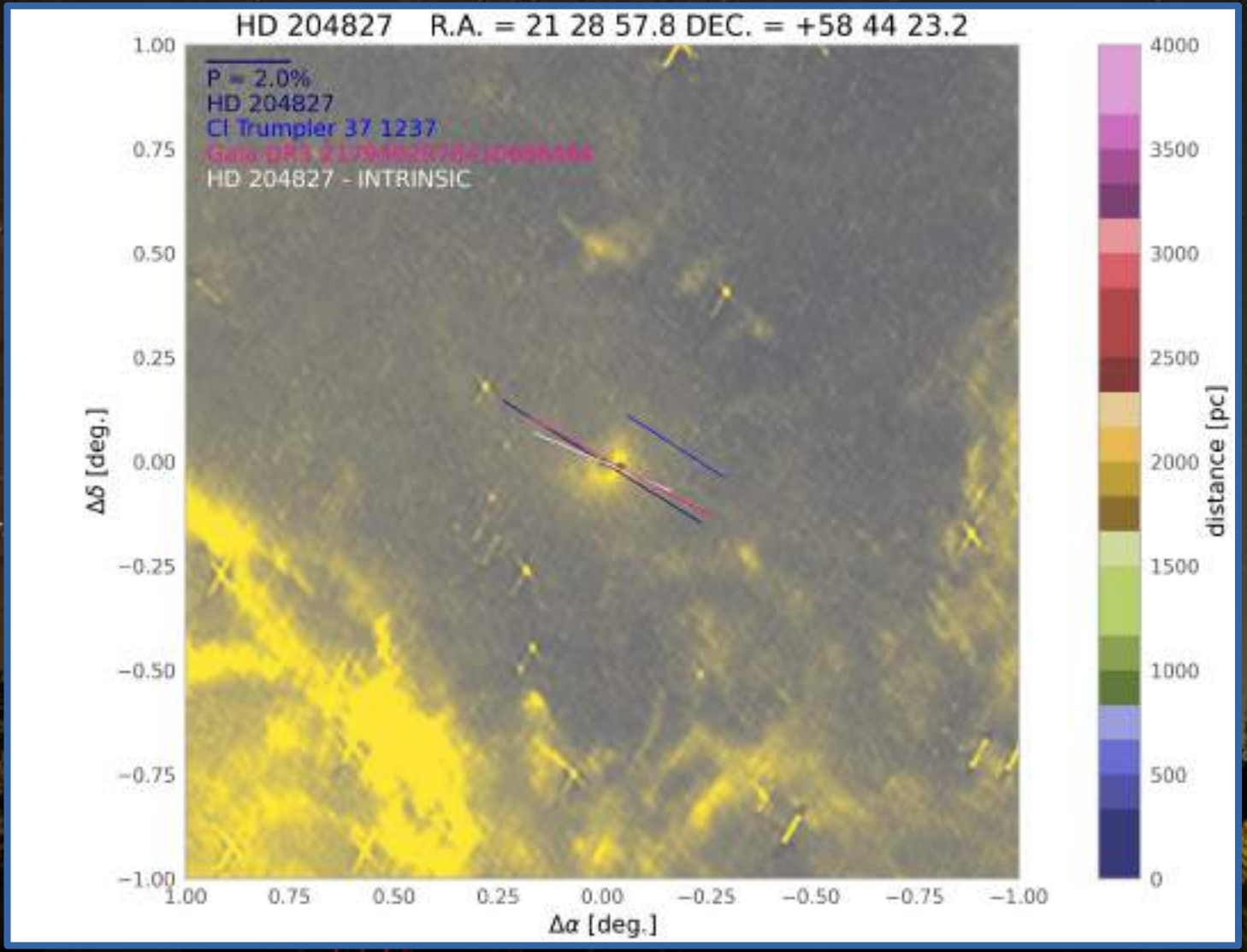

The position angles of HD 204827 and two nearby stars. The Stokes Q and U of CT Trumpler 37 1237 was used to calculate the intrinsic degree of polarization and position angle of HD 204827 (with blue). The background represent 25μm dust emission taken from HIRES (IRAS).

Nikolov in prep.

Променливост в степента на поляризация при HD 204827

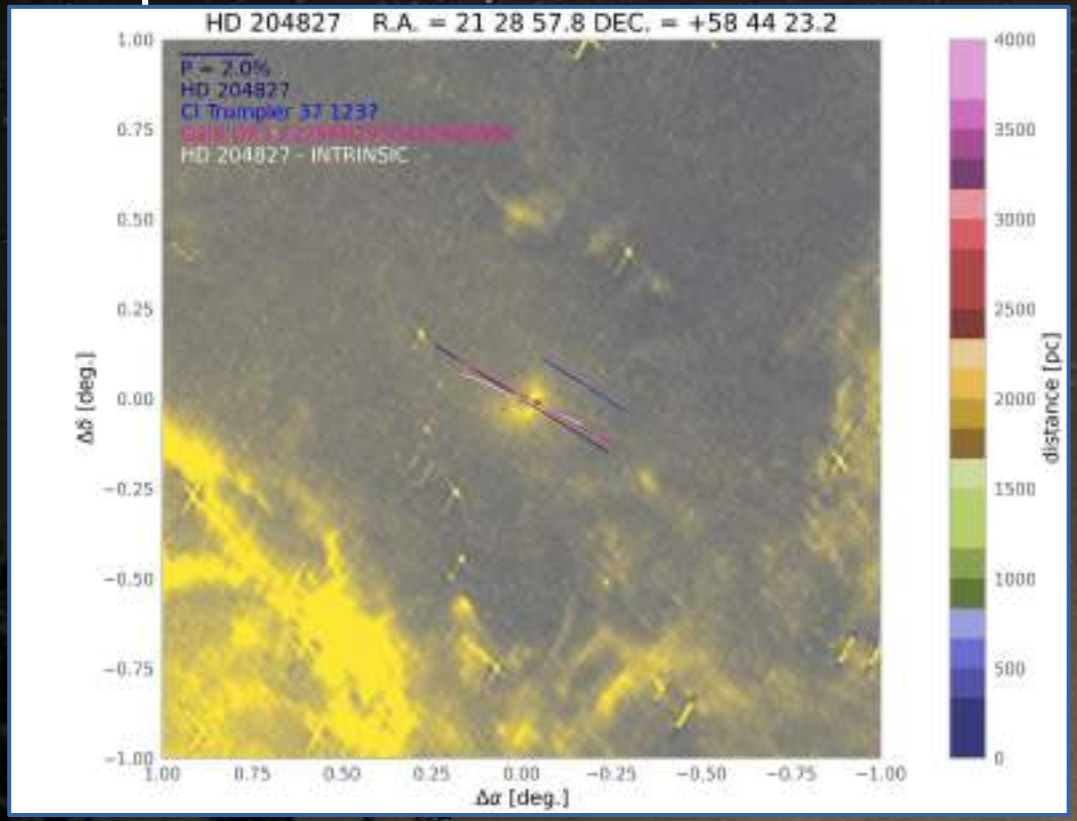

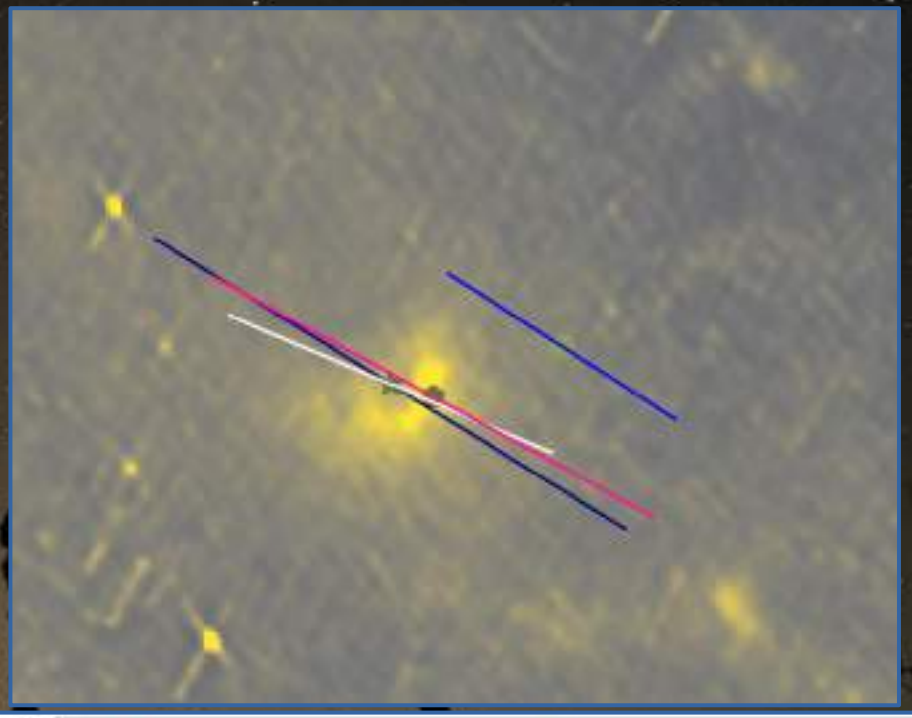

The position angles of HD 204827 and two nearby stars. The Stokes Q and U of CT Trumpler 37 1237 was used to calculate the intrinsic degree of polarization and position angle of HD 204827 (with blue). The background represent 25μm dust emission taken from HIRES (IRAS).

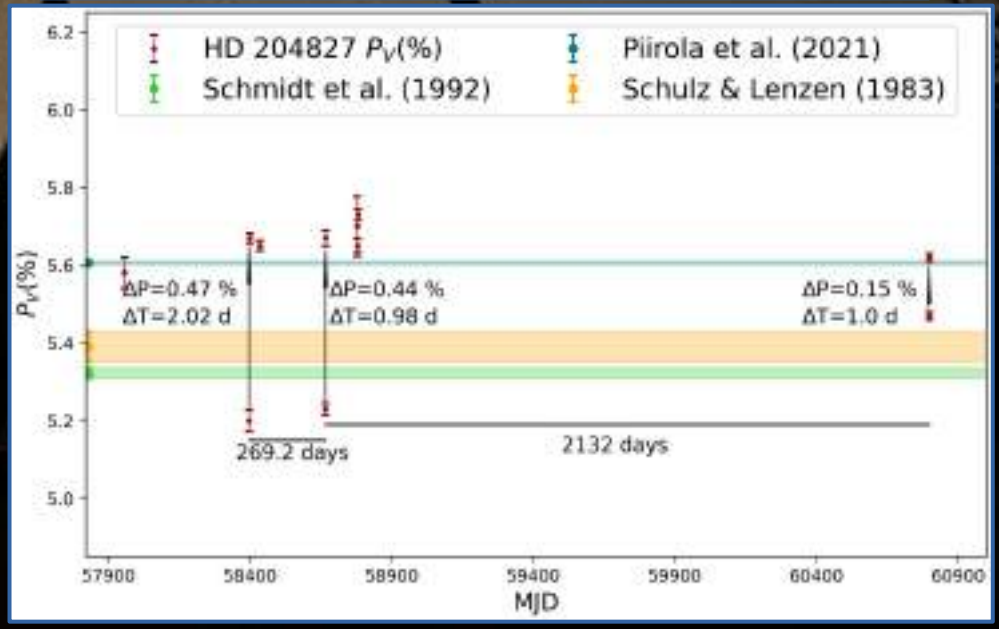

Long-term variability of HD 204827 in the synthetic V-band. The catalogue values are presented with horizontal lines, where the width of each line corresponds to the error of the catalogue value.

Благодаря за вниманието

Acknowledgements
This work was supported by Bulgarian National Science Fund of the Ministry of Education and Science under
grand:КП-06-М88/1 "Interstellar medium – 3D distribution and physical characteristics"

Rauch + 2013